Available online at www.sciencedirect.com
SCIENCE DIRECT
Catalysis Today 114 (2006) 346–352
CATALYSIS TODAY
www.elsevier.com/locate/cattod

Enantioselective hydrogenation of ethyl pyruvate catalysed by Pt/graphite: Superior performance of sintered metal particles

G.A. Attard [a,*], K.G. Griffin [b], D.J. Jenkins [a], P. Johnston [b], P.B. Wells [a,*]

[a] Department of Chemistry, Cardiff University, P.O. Box 912, Cardiff CF10 3TB, UK
[b] Johnson Matthey, Orchard Road, Royston, Herts SG8 5HE, UK

Available online 24 April 2006

Abstract

A 5% Pt/graphite catalyst has been sintered in 5% H_2/Ar at 400, 500, 600, 700, 800, and 1000 K and cinchonidine-modified samples used to catalyse enantioselective ethyl pyruvate hydrogenation at 293 K and 30 bar pressure. Changes in catalyst morphology on sintering have been investigated by high resolution electron microscopy and cyclic voltammetry. The as-received catalyst contained small Pt particles aggregated into clusters. As the temperature was raised these clusters disaggregated; the resulting small particles grew, first showing enhanced crystallinity and better defined step and terrace topography, and later progressive faceting. Ultimately the particles were large and hexagonal. These processes were accompanied by a loss of surface area and a reduction in catalytic activity. Enantiomeric excess rose from 43% for as-received material to 63% for catalyst sintered at 700 K, and declined for higher sintering temperatures. The particle size distribution for the optimal catalyst peaked at 8 nm and most particles were substantially faceted. Chiral performance is interpreted in terms of enhanced enantioselectivity provided by edge sites in the Pt surface. Modification of chiral kink sites by alkaloid, to give diastereomeric enantioselective sites may have further enhanced the enantioselectivity. The investigation provides clear objectives for future catalyst design.

Keywords: Enantioselective hydrogenation; Pyruvate ester; Pt/graphite; Sintered catalyst; Cyclic voltammetry; Step-site activity; Kink-site activity

1. Introduction

Enantioselective hydrogenation of ethyl pyruvate, other α-ketoesters, and related compounds by Pt catalysts modified by the adsorption of cinchona alkaloids onto their surfaces has been studied extensively since such reactions were first reported [1,2], and the main features of the mechanism are understood [3–5]. High values of the enantiomeric excess (>90%) have been reported, usually in special situations (e.g. stabilised colloidal particles [6], ultrasonicated catalyst [7], restructured catalyst [8]), but the performance of widely available catalysts is not sufficient to be attractive for industrial application. For example, in ethyl pyruvate hydrogenation to ethyl lactate over cinchonidine-modified catalysts, Pt/alumina regularly gives values of the enantiomeric excess in the range 75–85% (*R*) [5,9], Pt/silica 65–75% (*R*) [10,11], Pt/graphite 40–45% (*R*) [2,12,13] and Pt/carbon 20–40% (*R*) [2,14]. Mean Pt particle size is a relevant variable, the tendency for enantiomeric excess to increase with decreasing Pt dispersion has long been recognised [9]. Indeed, in their original study, Orito et al. improved the performance of Pt/C by heat treatment [2]. More recently, it has been proposed that the detailed morphology of the Pt surface (i.e. the relative populations of sites at terraces, steps and kinks in the surface) may determine performance such that the observed enantiomeric excess may be a weighted average of the values provided by all the constituent terrace and step features that make up the polycrystalline Pt surface [12,15]. If such is the case, then the challenge for the achievement of very high enantioselectivity becomes one of catalyst design.

To test this proposal cyclic voltammetry has been used to provide information concerning Pt particle morphology in supported Pt catalysts. Cyclic voltammograms (CVs) for Pt single crystal surfaces are well known, and Pt/graphite catalysts show four features that correspond (by analogy with the single crystal data) to Pt{1 1 1} × {1 1 1} steps, Pt{1 0 0} × {1 1 1} steps, Pt{1 0 0} terraces and Pt{1 1 1} terraces [12,16]. Thus changes in the populations of these surface features with

* Corresponding authors. Tel.: +44 2920 874069; fax: +44 2920 874030.
E-mail address: attard@cardiff.ac.uk (G.A. Attard).

0920-5861/$ – see front matter
doi:10.1016/j.cattod.2006.02.075

catalyst treatment can be investigated and the effects on catalytic activity and selectivity determined. Application of this technique is confined to conducting samples—hence the use of Pt/graphite; it cannot be used directly to study better-performing catalysts such as Pt/alumina and Pt/silica. However, where Pt/graphite and, say, Pt/silica show a common trend in catalytic behaviour an interpretation provided by cyclic voltammetry for Pt/graphite may be applicable by analogy to Pt/silica.

The first demonstration of the efficacy of this approach has been the use of Bi and S as site-blocking agents to determine the relative chiral efficiencies of step and terrace sites [12,13,15]. Bi adsorbed onto Pt/graphite selectively occupied step sites; only when step-site occupation was complete were terrace sites occupied. Modification of such bismuthated Pt catalysts by cinchonidine provided values of the enantiomeric excess in high pressure hydrogenation of ethyl pyruvate which decreased linearly with increasing Bi coverage from 42% (*R*) (no Bi) to 22% (*R*) (full step-site occupation by Bi); further addition of Bi then occurred at terrace sites and led to a small further decrease in enantiomeric excess. By contrast, adsorption of *S* occurred mainly though not exclusively on Pt terraces and enantiomeric excess increased from 42% (*R*) to 53% (*R*). These observations demonstrated clearly that enantioselective sites located in the vicinity of steps provided a higher enantiomeric excess than sites located on terraces. Such enhanced performance at step sites may simply arise because of improved access of pyruvate ester to the chiral environment of the adsorbed alkaloid when the dimensionality of the enantioselective site is increased from two to three.

Comparable behaviour was observed when Bi was adsorbed onto Pt/silica; enantiomeric excess fell from 74% (*R*) to 21% (*R*) with increasing Bi coverage and reduced only slowly thereafter. Thus (by analogy) the step sites on the (smaller) Pt particles in Pt/silica were apparently more enantioselective than those on the (larger) Pt particles in Pt/graphite.

A further demonstration of the differential chiral efficiencies of step and terrace sites should be obtainable by an examination of the effects of thermal annealing and sintering the Pt/graphite catalyst. In general, thermal annealing and sintering induce reconstruction and growth of Pt particles resulting in a change in the balance of steps and terraces. In this investigation, sintered 5% Pt/graphite catalysts have been characterised and the consequential effects on enantioselectivity observed.

2. Experimental

About 5% Pt/graphite (Pt area 2.1 $m^2\ g^{-1}$) was supplied by Johnson Matthey. Six samples of sintered catalyst were prepared as follows. For each sample, 1–2 g Pt/graphite was placed in a silica boat in a tube furnace at ambient temperature and air expelled by a flow of Ar for 0.3 h. The gas flow was then switched to 5% H_2/Ar and the temperature raised at 10 K min^{-1} to the required sintering temperature; this temperature was maintained for 3 h after which the samples were allowed to cool naturally to room temperature in the H_2/Ar stream and were then exposed to air. Sintering temperatures investigated were 400, 500, 600, 700, 800, and 1000 K. Samples were examined by high resolution transmission electron microscopy (Johnson Matthey laboratories, Philips FEI Technai-F20, 200 kV, 0.15 nm resolution). Catalysts, including the as-received material, required no re-reduction before use.

The two-component electrochemical cell used for catalyst characterisation has been described [17]. The working electrode was a Pt basket containing about 2.7 mg catalyst, the electrolyte was 0.5 M sulphuric acid, voltage was swept between 0 and 0.8 V at a rate of 10 mV s^{-1}. Cyclic voltammograms showed electrosorption peaks at 0.06, 0.20, 0.28, and 0.47 V attributed (by comparison with single crystal data [15]) to the presence of $\{1\ 1\ 1\}_{terr} \times \{1\ 1\ 1\}_{step}$ step sites, $\{1\ 0\ 0\}_{terr} \times \{1\ 1\ 1\}_{step}$ step sites, {1 0 0} terraces and {1 1 1} terraces, respectively [16]. The area under the voltammograms was reduced when sintering resulted in a loss of Pt surface area; the measurement for the as-received material was given the value 100 and values for other samples were scaled accordingly.

Catalyst samples were rendered enantioselective by in situ modification with cinchonidine. Typically, 65 mmol (7.2 ml) ethyl pyruvate, 0.17 mmol (50 mg) cinchonidine, catalyst (0.25 g) and dichloromethane solvent (12.5 ml) were measured into the glass-lined reactor in that order. The reactor was sealed, purged several times with hydrogen to remove air, pressurised to 30 bar, and the stirrer started immediately whereupon reaction commenced. A Büchi 9204 gas dosing system admitted hydrogen to compensate for that consumed and provided uptake/time data so that rate and conversion could be observed. Reactions were of the usual type [10,15] consisting of a mild initial acceleration, followed by a sustained period of reaction at maximum rate, and finally a deceleration as reactant became exhausted. Activity measurements recorded below correspond to measurements of the maximum rate. All reactions were taken to 90–100% conversion. Product analysis was by chiral gas–liquid chromatography (25 m capillary column, chiral β-cyclodextrine stationary phase (Varian)). Ethyl pyruvate hydrogenations produced *R*- and *S*-ethyl lactate together with small yields of a pyruvate-lactate adduct described elsewhere [15]. Enantiomeric excess is defined as usual as $([R\text{-}] - [S\text{-}])10^2/([R\text{-}] + [S\text{-}])$. All reactions showed an enantiomeric excess in favour of the *R*-product; the uncertainty in the quoted values was ±1%.

3. Results

3.1. Characterisation of sintered Pt/graphite

Fig. 1a shows an electron micrograph and Fig. 2a the cyclic voltammogram of as-received Pt/graphite. The Pt active phase existed as small particles aggregated into large irregular clusters as is typical for carbon- and graphite-supported Pt prepared by liquid-phase reduction. The CV showed the presence of the two-step features and the two terrace features described above. The effects on particle morphology and crystallinity of heating individual samples of as-received Pt/graphite to 400, 500, 600, 700, 800, and 1000 K are set out in Tables 1–3 and examples illustrated in Figs. 1 and 2. The area

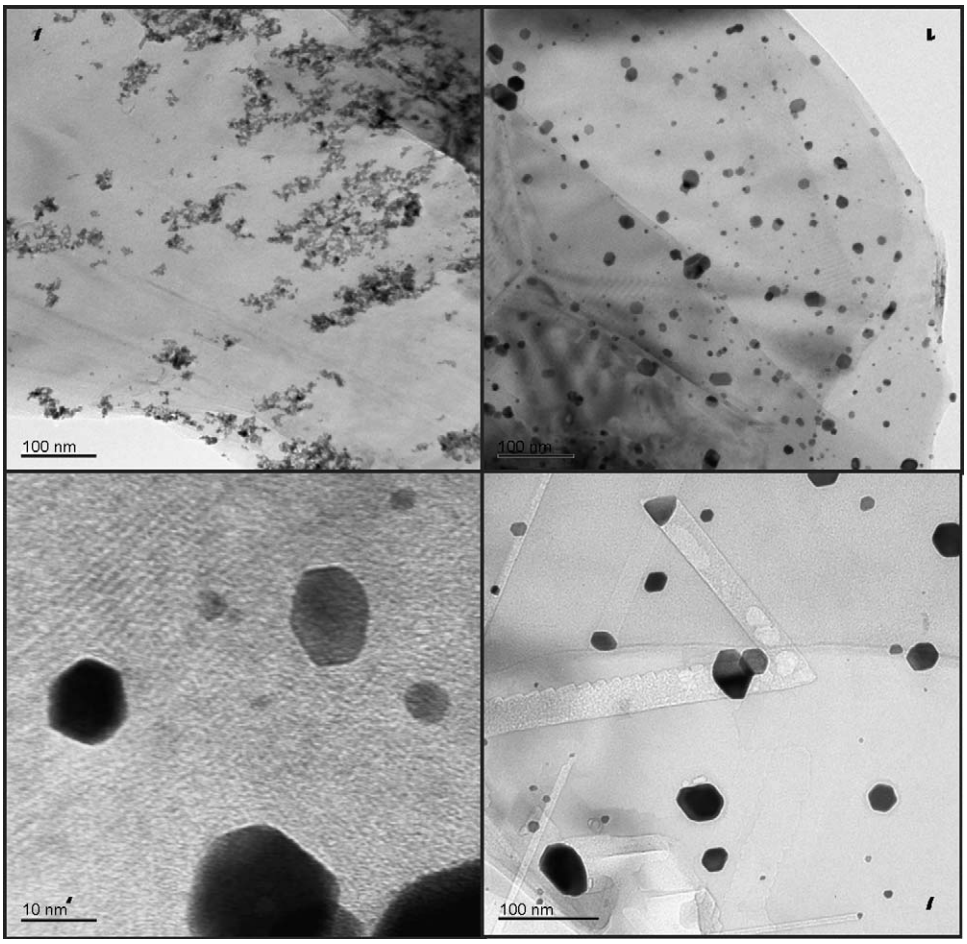

Fig. 1. Electron micrographs of Pt/graphite: (a) [top left] as-received, (b) [top right] sintered at 700 K; (c) [bottom left] sintered at 700 K (10× higher linear magnification); (d) [bottom right] sintered at 1000 K. Magnifications: for (a), (b), and (d) the bar represents 100 nm; (c) the bar represents 10 nm.

under the electrosorption peaks decreased with increasing sintering temperature indicating a loss of Pt surface area (Table 1). Table 2 indicates that irregular clusters of small Pt particles that pre-existed in the as-received material (Fig. 1a) largely survived heating to 400 K but became more uniform in appearance and showed clearer boundaries. The irregular clusters had mostly disaggregated at 500 K and none survived to 600 K. Disaggregation of irregular clusters generated small spheroidal particles which grew in size with increasing temperature giving larger spheroidal particles which then developed facets. Fig. 1b shows the catalyst sintered at 700 K in which faceting is well-advanced. In Fig. 1c the underlying

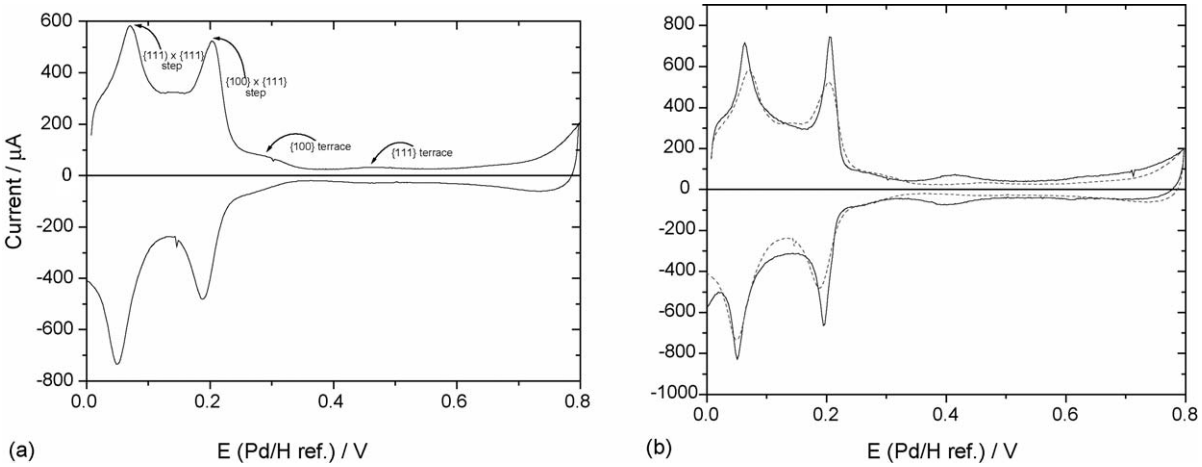

Fig. 2. Cyclic voltammograms of Pt/graphite: (a) as-received, (b) sintered at 700 K (full curve). Part (b) show both the CV for the 700 K sintered sample (full curve) and that for the as-received catalyst (dashed curve), the curves having been normalised to take account of the loss of area of the sintered sample.

Table 1
Effects of sintering 5% Pt/graphite on relative Pt area, and on catalytic activity and enantiomeric excess for ethyl pyruvate hydrogenation at 30 bar and 293 K

Sintering temp (K)	Not heated	400	500	600	700	800	1000
Relative Pt area[a]	100	59	35	34	29	24	10
Activity (pyruvate)[b]	830	370	160	160	40	20	Very slow
Enantiomeric excess/% (*R*)[c]	43	45	56	59	63	57	38

[a] Determined by cyclic voltammetry.
[b] Units: mmol h^{-1} g^{-1}.
[c] Value for sample sintered at 1000 K obtained by increasing catalyst sample size to 0.49 g and analysing after 90% conversion.

Table 2
Effects of sintering 5% Pt/graphite on Pt particle shape and size as determined by electron microscopy

Sintering temp (K)	Not heated	400	500	600	700	800	1000
Particle appearance							
Irregular clusters	All	Most	Many				
Spheroidal particles		Few	Many	Few	Few		
Faceted particles			Few	Most[a]	Most	All	All[b]
Size of most abundant particles/nm				6	8	10	30

[a] Some irregular hexagonal particles.
[b] Many regular hexagonal particles.

Table 3
Effects of sintering 5% Pt/graphite on Pt particle morphology as determined by cyclic voltammetry

Sintering temp (K)	Not heated	400	500	600	700	800	1000
Particle morphology							
{1 1 1} × {1 1 1} step feature (0.06 V)	Present	Slightly broader	Narrower	No change	More intense	More intense	Less intense
{1 0 0} × {1 1 1} step feature (0.20 V)	Present	Less intense	More intense	Slightly narrower	More intense	Less intense	More intense
{1 0 0} terrace feature (0.28 V)	Present	No change	More intense	Additional intensity lost	No change	No change	No change
{1 1 1} terrace feature (0.47 V)	Present	More intense	More intense	No change	More intense	Sl. less intense	No change

texture of the graphite support is visible beneath these hexagonal particles, showing that they were very thin. Above 700 K particle growth continued and the extent of faceting increased so that, after heating at 1000 K, the particles were mostly large and of hexagonal appearance (Fig. 1d). Particle size distributions were obtained for samples not containing irregular clusters; that for the 700 K sintered catalyst is shown in Fig. 3. Values of most abundant particle size are recorded in Table 2. The effect of sintering temperature on surface crystallinity is presented in Table 3. In order to discern changes in morphology, the CVs of the sintered samples were scaled to take account of loss of area and compared with the CV for the as-received material. An example of such comparative CVs is given in Fig. 2b. An increase in the intensity of a feature in the CV is indicative of an increase in the surface population of that step or terrace, whereas a feature that narrows is indicative of increased long range order in the surface.

Table 3 shows that heating at 400 K, which caused a change in the appearance of the irregular clustered particles, was accompanied by an increase in the concentration of {1 1 1} terraces, a small diminution in the density of {1 0 0} × {1 1 1} steps, and in the long range order of {1 1 1} × {1 1 1} steps. The catalyst heated to 500 K exhibited a marked increase in crystallinity which accompanied the formation of substantial numbers of small spheroidal particles. These particles also showed enhanced {1 0 0} terraces. The interval from 500 to 600 K was remarkable for the onset of faceting and the loss of the additional intensity that had developed in the {1 0 0} terrace feature. Further increases in crystallinity (densities of both steps and the {1 1 1} terraces with no re-emergence of {1 0 0} terraces) occurred on heating to 700 K and this was

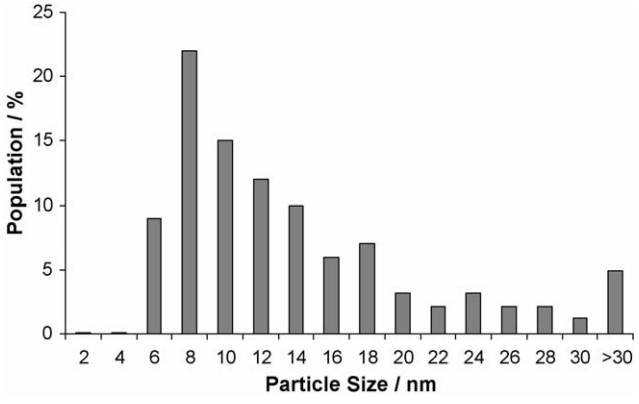

Fig. 3. Pt particle size distribution in Pt/graphite sintered at 700 K as measured by electron microscopy (instrumental measurement).

accompanied by further faceting. Heating to 800 and 1000 K led to various changes in step densities and there was a general increase in crystallinity as the Pt particles became very large and regularly hexagonal (Fig. 1d).

Thus, sintering in 5% H_2/Ar involved three processes (i) disaggregation of pre-existing irregularly clustered particles to give isolated small spheroidal particles under conditions where the overall degree of crystallinity progressively increased, (ii) spheroidal particle growth with further improved crystallinity and loss of {1 0 0} terraces, and (iii) faceting of particles and further growth until most particles were large and regularly faceted.

3.2. Catalytic performance of sintered Pt/graphite

Table 1 shows how activity for enantioselective ethyl pyruvate hydrogenation over cinchonidine-modified sintered catalysts declined as the Pt surface area diminished. Heating to 400 K (which caused a change in the appearance of the aggregates) was accompanied by a reduction in activity of 55% and by a marginal improvement in enantiomeric excess from 43% to 45% (Fig. 4).

This dramatic activity loss is consistent with the effect of heating to 400 K being one of thermal annealing. Partial disaggregation of the irregularly clustered particles and improved surface order on heating to 500 K induced a substantial improvement in enantiomeric excess from 45% to 56%. Complete disaggregation, loss of {1 0 0} terraces, and the commencement of faceting which occurred on heating to 600 K produced an improvement in enantiomeric excess to 59%. Finally, the best chiral performance (ee = 63%) was obtained after heating to 700 K when faceting of modest-sized particles was extensive. Further particle growth over the range 800 to 1000 K led to a decline in enantiomeric excess.

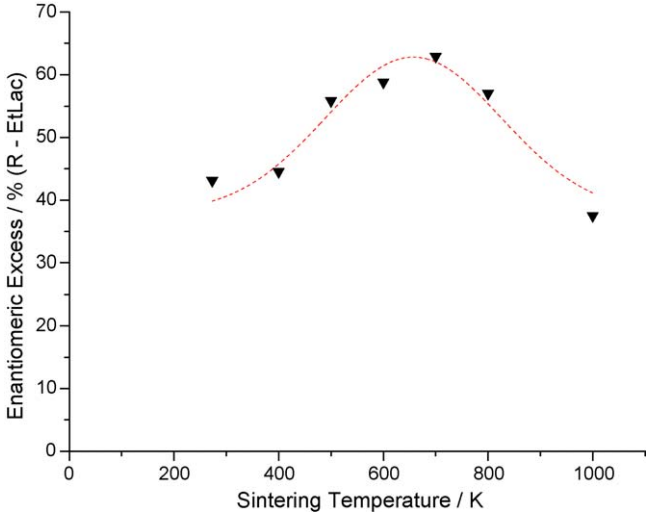

Fig. 4. High pressure ethyl pyruvate hydrogenation over cinchonidine-modified Pt/graphite catalysts: variation of enantiomeric excess with sintering temperature under standard conditions (see Section 2).

4. Discussion

The widely-accepted mechanism for the enantioselective hydrogenation of pyruvate esters over cinchonidine-modified Pt is one in which cinchonidine molecules in the open-3 conformation are adsorbed at a Pt surface and ethyl pyruvate is adsorbed by one or other of its enantiofaces in the 'chiral cleft' of the adsorbed alkaloid [3,4,11]. Hydrogenation of molecules adsorbed by one enantioface provides *R*-lactate as product whereas hydrogenation of molecules adsorbed by the other enantioface provides *S*-lactate. Alkaloid–reactant interactions are such that *R*-lactate is formed preferentially at enantioselective sites created by the adsorption of cinchonidine on Pt surfaces. Correspondingly, the near-mirror-image alkaloid cinchonine provides preferential formation of *S*-lactate. The molecular arrangements have been presented as involving adsorption on {1 1 1} planes and about 25 surface Pt atoms in a two-dimensional array are required to achieve the required 1:1 alkaloid–reactant interaction [11].

Sintering at 400 K produced a 55% decrease in activity but little change in enantiomeric excess, indicating that thermal annealing of the metastable Pt particles formed by low temperature liquid-phase reduction did not influence the type of enantioselective site available at the surface.

The rise in enantiomeric excess from 45% to 56% on increasing sintering temperature from 400 to 500 K demonstrates that the accompanying increase in crystallinity provided a surface better able to accommodate the 1:1 alkaloid–reactant complexes in an optimum configuration. This may have been achieved both by an increase in the number of ~25-atom arrays on flat surfaces such as {1 1 1} terraces and by an increase in the number of such arrays at near-step locations which are known, from Bi deposition studies, to provide enhanced values of the enantiomeric excess [12,13].

Either continuously increasing crystallinity or the advent of faceting (or both) contributed to the increase in enantiomeric excess from 56% to 63% on raising sintering temperature from 500 to 700 K. Increasing crystallinity is unlikely to have been the main factor because it continued above 700 K where enantiomeric excess fell. However, a favourable association of enantiomeric excess with faceting is expected, providing the facets observed contribute to the types of step sites at which enhanced enantioselectivity is achieved.

On progressing from 700 to 800 K enantiomeric excess fell from 63% to 57%, which suggests that particle growth resulted in fewer step sites as a proportion of the total number of surface sites present. 700 K is about one-third of the Pt melting point above which significant surface diffusion is expected to occur (Huttig's Rule); this may have led to a slight reduction in step-site concentration at 800 K which was evident in terms of catalytic performance though not detectable in the CV.

The sample sintered at 1000 K gave an enantiomeric excess lower than that of the as-received catalyst (Table 1). The micrograph showed tracks in the graphite support (Fig. 1d) attributable to movement of the Pt particles and the CV indicated that the Pt phase was contaminated. These observations suggest the occurrence of active metal-support chemistry

at 1000 K causing C-contamination of the Pt surface and a reduction in subsequent catalytic performance.

Another factor having the potential to relate facet structure and particle size to enantiomeric excess concerns the chiral nature of kink sites formed at points where steps intersect [15,18–22]. Kink sites in chiral Pt single crystal surfaces, Pt(6 4 3) is an example, are formed by the intersection of {1 1 1}, {1 0 0}, and {1 1 0} elements; *R*-kinks consist of a clockwise sequence of such elements whereas *S*-kinks consist of an anticlockwise sequence. Accordingly, single crystal surfaces with only *R*- or *S*-kink sites can be grown and chiral recognition at such inherently optically active surfaces has been observed in the context of electrochemical D- and L-glucose oxidation [18,23,24]. No chiral recognition was evident, however, in the adsorption of cinchonidine or cinchonine [25]. In supported Pt catalysts, the random growth mode of the metal microcrystals during preparation and sintering should ensure that, whatever the population of these types of chiral site, the concentration of *R*-kinks will be compensated by an identical concentration of *S*-kinks. For supported catalysts there is the additional possibility of implicit chirality at points where faceted metal particles contact the support surface [15]. Fig. 5a shows an hexagonal bi-layer of Pt atoms. At each corner of the hexagon there are three coincident {1 1 1}, {1 0 0} and [support] elements, such that (using the convention for chirality in homogeneous crystals) the corners can be described as having alternate *R*- and *S*-character, as shown.

Where optically active alkaloid molecules (*R*-cinchonidine for present purposes) adsorb at *R*- and *S*-kink sites, whether on the extended Pt surface or at the particle-support interface, the resulting enantioselective sites acquire diastereomeric character resulting in the creation of two different chiral environments (*R*-alkaloid at *R*-kinks, and *R*-alkaloid at *S*-kinks). Ethyl pyruvate molecules may respond to these diastereo-environments either by reacting at different rates and/or by providing different values of the enantiomeric excess in the hydrogenated product. Thus, there may be implications for chiral outcome, even where the populations of *R*- and *S*-kink sites are the same.

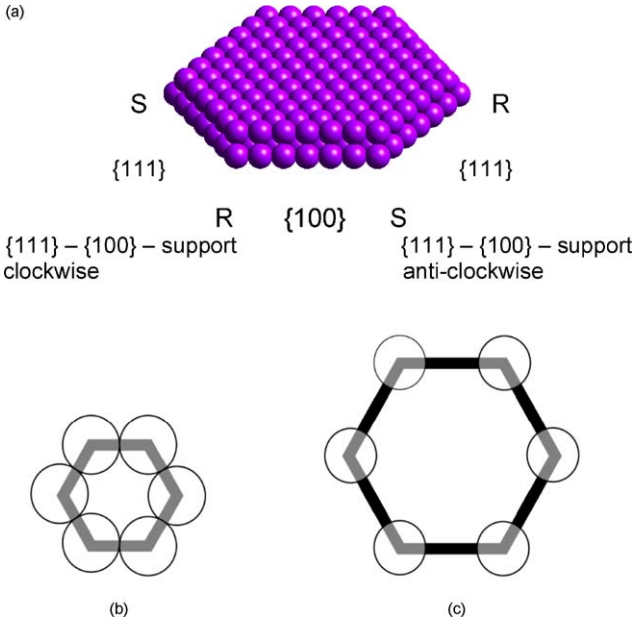

Fig. 5. (a) A schematic presentation of an hexagonal bi-layer of Pt atoms on a support surface, showing the edge structures which define chirality at the kink sites; (b) optimum arrangement of diastereoisomeric enantioselective sites (open circles) formed by alkaloid adsorption at the chiral kink sites around an hexagonal Pt particle; (c) non-optimum arrangement of such sites around a larger Pt particle.

Whether chiral site participation influenced enantiomeric excess in the present study is uncertain. Such sites would be present at maximum concentration in hexagonal particles of about 5 nm in size (Fig. 5b) (presuming these enantioselective sites also require the availability of arrays of about ∼25 Pt surface atoms). A test would require the preparation of catalysts having faceted particles with a narrow size distribution centred at ∼5 nm. Chiral site participation would then be evident from a decline in enantiomeric excess with increasing particle size on further sintering, as both step sites at faceted edges between kinks and step and terrace sites in non-edge situations made larger contributions to overall reaction (Fig. 5c). Promotion of such geometrically optimised catalysts might then be achievable by selective blocking of less enantioselective sites in non-edge locations, as has been achieved for our as-received Pt/graphite catalyst using S^{2-} adsorption [12,13].

Finally, the particle size distribution for the 700 K sintered catalyst was wide and showed a maximum at 8 nm (Fig. 3). By comparison, unsintered EUROPT-1 has a narrow size distribution (1.5–3.5 nm) centred at 2 nm [26] and shows superior chiral performance (ee ∼70% [11]). Future work will concentrate on the preparation of Pt/graphites containing smaller faceted Pt particles with a narrow size distribution, containing only step sites that have the appropriate geometry for efficient modification by alkaloid.

5. Conclusions

Changes in morphology and accompanying changes in enantioselective performance of Pt particles in progressively sintered Pt/graphite catalysts have been observed and interpreted in terms of the known superior chiral performance of catalyst sites in edge situations. The possibility that chiral kink sites raise enantiomeric excess via the creation of diastereomeric sites has been rehearsed and awaits further experimental test. The enantiomeric excess of 63% given by the present catalyst sintered in H_2/Ar at 700 K is considered to be the best attainable without recourse to promotion by site-blocking agents.

Acknowledgments

We thank the EPSRC and Johnson Matthey for financial support for DJJ.

References

[1] Y. Orito, S. Imai, S. Niwa, in: Proceedings of the 43rd Catal. Forum Jpn., 1978, p. 30.

[2] Y. Orito, S. Imai, S. Niwa, Nippon Kagau Kaishi, 1979, p. 1118.
[3] A. Baiker, J. Mol. Catal. A: Chem. 115 (1997) 473.
[4] P.B. Wells, R.P.K. Wells, in: D.E. De Vos, I.F.J. Vankelecom, P.A. Jacobs (Eds.), Chiral Catalyst Immobilisation and Recycling, Wiley-VCH, Weinheim, 2000, p. 123.
[5] M. Studer, H.-U. Blaser, C. Exner, Adv. Syn. Catal. 345 (2003) 45.
[6] X.I. Zuo, H. Liu, M. Liu, Tetrahedron Lett. 39 (1998) 1941.
[7] B. Toeroek, K. Balazsik, M. Toeroek, K. Felfoldi, M. Bartok, Catal. Lett. 81 (2002) 55.
[8] R. Hess, F. Krumeich, T. Mallat, A. Baiker, Catal. Lett. 92 (2004) 141.
[9] J.T. Wehrli, A. Baiker, D.M. Monti, H.-U. Blaiser, J. Mol. Catal. 61 (1990) 207.
[10] I.M. Sutherland, A. Ibbotson, P.B. Wells, J. Catal. 128 (1991) 387.
[11] K.E. Simons, P.A. Meheux, S.P. Griffiths, I.M. Sutherland, P. Johnston, P.B. Wells, A.F. Carley, M.K. Rajumon, M.W. Roberts, A. Ibbotson, Recl. Trav. Chim. Pays-Bas 113 (1994) 465.
[12] G.A. Attard, D.J. Jenkins, O.A. Hazzazi, P.B. Wells, J.E. Gillies, K.G. Griffin, P. Johnston, Catalysis in Application, Royal Society of Chemistry, Cambridge, 2003, p. 70.
[13] D.J. Jenkins, A.M.S. Alabdulrahman, G.A. Attard, K.G. Griffin, P. Johnston, P.B. Wells, J. Catal. 234 (2005) 230.
[14] M.A. Fraga, M. Meules, E.J. Jordao, J. Mol. Catal. A: Chem. 179 (2002) 243.
[15] G.A. Attard, A. Ahmadi, D.J. Jenkins, O.A. Hazzazi, P.B. Wells, K.G. Griffin, P. Johnston, J.E. Gillies, Phys. Chem. Chem. Phys. 4 (2003) 123.
[16] G.A. Attard, J.E. Gillies, C.A. Harris, D.J. Jenkins, P. Johnston, M.A. Price, D.J. Watson, P.B. Wells, Appl. Catal. A: General 222 (2001) 393.
[17] R.W. Evans, G.A. Attard, J. Electroanal. Chem. 345 (1993) 337.
[18] A. Ahmadi, G.A. Attard, J. Feliu, A. Rhodes, Langmuir 15 (1999) 2420.
[19] G.A. Attard, A. Ahmadi, J. Feliu, A. Rhodes, E. Herrero, S. Blais, G. Jerkiewicz, J. Phys. Chem. B 103 (1999) 1381.
[20] G.A. Attard, J. Clavilier, J.M. Feliu, in: J.M. Hicks (Ed.), Chirality: Physical Chemistry, ACS Sump. Ser. 801, ACS Publications, Washington DC, 2002, p. 254.
[21] C.F. McFadden, P.S. Cremer, A.J. Gellman, Langmuir 12 (1999) 2483.
[22] T. Power, D.S. Sholl, Top. Catal. 18 (2002) 201.
[23] G.A. Attard, J. Phys. Chem. B 105 (2001) 3158.
[24] G.A. Attard, C. Harris, E. Herrero, J. Feliu, Faraday Discuss. 121 (2002) 253.
[25] O.A. Hazzazi, G.A. Attard, P.B. Wells, J. Mol. Catal. A: Chem. 216 (2004) 247.
[26] J.W. Geus, P.B. Wells, Appl. Catal. 18 (1985) 231.